

Influence of environmental changes on the biogeochemistry of arsenic in a soil polluted by the destruction of chemical weapons: A mesocosm study

Hugues Thouin, Fabienne Battaglia-Brunet, Marie-Paule Norini, Lydie Le Forestier, Mickael Charron, Sébastien Dupraz, Pascale Gautret

▶ **To cite this version:**

Hugues Thouin, Fabienne Battaglia-Brunet, Marie-Paule Norini, Lydie Le Forestier, Mickael Charron, et al.. Influence of environmental changes on the biogeochemistry of arsenic in a soil polluted by the destruction of chemical weapons: A mesocosm study. Science of the Total Environment, 2018, 627, pp.216-226. 10.1016/j.scitotenv.2018.01.158 . insu-01700628

HAL Id: insu-01700628
https://insu.hal.science/insu-01700628

Submitted on 12 Feb 2018

HAL is a multi-disciplinary open access archive for the deposit and dissemination of scientific research documents, whether they are published or not. The documents may come from teaching and research institutions in France or abroad, or from public or private research centers.

L'archive ouverte pluridisciplinaire **HAL**, est destinée au dépôt et à la diffusion de documents scientifiques de niveau recherche, publiés ou non, émanant des établissements d'enseignement et de recherche français ou étrangers, des laboratoires publics ou privés.

Influence of environmental changes on the biogeochemistry of arsenic in a soil polluted by the destruction of chemical weapons: a mesocosm study

Hugues Thouin [a,b,c,d], Fabienne Battaglia-Brunet [a,b,c,d], Marie-Paule Norini [b,c,d], Lydie Le Forestier [b,c,d], Mickael Charron [a], Sébastien Dupraz [a] and Pascale Gautret [b,c,d]

[a] BRGM, 3 avenue Claude Guillemin, 45060 Orléans, France

[b] Université d'Orléans, ISTO, UMR 7327, 45071 Orléans, France

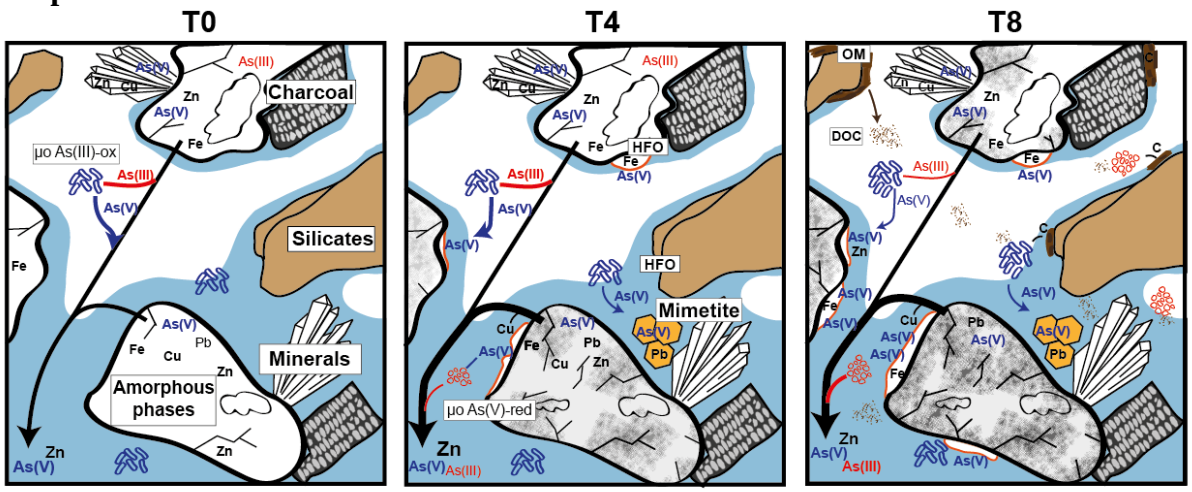
[c] CNRS, ISTO, UMR 7327, 45071 Orléans, France

[d] BRGM, ISTO, UMR 7327, BP 36009, 45060 Orléans, France

Highlights

- The surface of the main As, Cu and Zn carrier was alterated in water saturated conditions
- Precipitation of As(V)-bearing mineral mimetite contributed to the immobilization of As and Pb
- The addition of OM contributed to the growth of As transformation microorganisms
- As(III)-oxidizing activity was decreased by OM but remained the major As transformation phenomenon in the system.

Graphical abstract



Abstract

Thermal destruction of chemical munitions from World War I led to the formation of a heavily contaminated residue that contains an unexpected mineral association in which a microbial As transformation has been observed. A mesocosm study was conducted to assess the impact of water saturation episodes and input of bioavailable

organic matter (OM) on pollutant behavior in relation to biogeochemical parameters. Over a period of about eight (8) months, the contaminated soil was subjected to cycles of dry and wet periods corresponding to water table level variations. After the first four (4) months, fragmented litter from the nearby forest was placed on top of the soil. The mesocosm solid phase was sampled by three rounds of coring: at the beginning of the experiment, after four (4) months (before the addition of OM), and at the end of the experiment. Scanning electron microscopy coupled to energy dispersive X-ray spectroscopy observations showed that an amorphous phase, which was the primary carrier of As, Zn, and Cu, was unstable under water-saturated conditions and released a portion of the contaminants in solution. Precipitation of a lead arsenate chloride mineral, mimetite, in soils within the water saturated level caused the immobilization of As and Pb. Mimetite is a durable trap because of its large stability domain; however, this precipitation was limited by a low Pb concentration inducing that high amounts of As remained in solution. The addition of forest litter modified the quantities and qualities of soil OM. Microbial As transformation was affected by the addition of OM, which increased the concentration of both As(III)-oxidizing and As(V)-reducing microorganisms. The addition of OM negatively impacted the As(III) oxidizing rate, however As(III) oxidation was still the dominant reaction in accordance with the formation of arsenate-bearing minerals.

Keywords: Arsenic, metal, mineral stability, microbial arsenic transformation, organic matter, dry/wet cycles, mesocosm study

1. Introduction

At the end of the First World War (1914-1918), the former combatants had large stockpiles of unfired munitions. These unspent weapons were dismantled to recycle reusable material, then destroyed or abandoned by ocean dumping or land burial. Chemical weapons containing nitroaromatic, chlorine, bromine or arsenical compounds were destroyed primarily by burning because of their hazardous nature. The site called "Place-à-Gaz", located northeast of Verdun (France), is one of many sites along the western front line where chemical shells were destroyed. Between 1920 and 1928, approximately 200,000 shells containing organo-arsenic compounds were subjected to simple thermal treatment (Bausinger et al., 2007). The burnt munitions were primarily "blue cross shells" filled with arsenic-bearing vomiting agents CLARK I (diphenylchloroarsine) and CLARK II (diphenylcyanoarsine).

Thermal treatment resulted in severe As and heavy metal contamination of the upper 10 - 40 cm of topsoil at the site (Bausinger et al., 2007; Thouin et al., 2016). The surface layer where the inorganic contaminants are concentrated corresponds to the combustion residues of the munitions. This layer, composed of slag, scoria, various munitions elements, and large amounts of ash and charcoal from the firewood used for burning, is black in color (Bausinger et al., 2007; Thouin et al., 2016). The central part of the site was heavily contaminated with As, Zn, Cu, and Pb; concentrations of these elements reached 72,820 $mg.kg^{-1}$, 90,190 $mg.kg^{-1}$, 9,113 $mg.kg^{-1}$ and 5,777 $mg.kg^{-1}$, respectively (Thouin et al., 2016). Most organo-arsenic agents/compounds were oxidized during combustion, resulting in the release of inorganic arsenic As_2O_3 and As_2O_5 (Bausinger et al., 2007). A previous study by Thouin et al., (2016) showed that As was principally present as the pentavalent form (As(V)) within the solid phases (about 98 % of arsenate and 2 % of arsenite (As(III))) and that several arsenate minerals (adamite-olivenite series and pharmacosiderite) crystallized as the material cooled. An amorphous phase rich in Fe, Zn, Cu, and As and presenting a vitreous texture was also observed, highlighting the association of this unusual mineral assemblage with thermal treatment.

Microorganisms actively contributing to the metabolism of carbon and arsenic were detected at the site despite low organic matter (OM) bioavailability (Thouin et al., 2016). Microbial activity plays a major role in As speciation in soils (de Mello et al., 2007; Yamamura et al., 2009). For example, in mining environment, microbial As-transforming activity was used in biomining of As-bearing minerals and to clean up post mining contamination (Drewniak and Sklodowska 2013). Several bacterial mechanisms are responsible for As(III) oxidation or As(V)

reduction (Battaglia-Brunet et al., 2002; Bachate et al., 2012; Zobrist et al., 2000; Stolz et al., 2002), thus driving As mobility and bioavailability. Changes in environmental conditions, such as modifications of Eh or pH, are likely to modify these microbial activities. Moreover, the concentration and the composition of soil OM affect a microorganism diversity and biomass (Tiedje et al., 1999) and may impact bacterial As transformation (Bachate et al., 2012; Lescure et al., 2016). The cyclic saturation of soils was shown to induce the mobility and change of speciation of arsenic in relation with bacterial activities. Fe and As reduction and release were observed during flooding of contaminated soil (Weber et al., 2010) or redox oscillations (Couture et al., 2015). As-transforming microbes contribute actively to the transformation of As species in frequently saturated soils such as paddy fields (Xiao et al, 2016). However, up to now, the activity of As(III)-oxidizing and As(V)-reducing microorganisms has not been evaluated in highly polluted environments presenting the particular structure and composition of the weapon burning sites, and submitted to fluctuating water regimes.

The contaminated soil at the "Place-à-Gaz" site is regularly subjected to partial water saturation during periods of high precipitation and runoff because of the underlying clayey formation. Moreover, the margin of the site near the oak forest is exposed to natural deposition of litter that provides bioavailable OM. These environmental variations are capable of altering the carriers phases of As and affect bacterial As transformation activities, thereby changing As mobility at the site.

With the aim to better understand the cycle of As in this highly polluted material submitted to environmental changes, an eight-month experiment was performed in a 1 m^3 mesocosm filled with contaminated material that was subjected to water saturation episodes and input of bioavailable OM. Monitoring of interstitial water composition at different/various depths in the mesocosm and of leachate (outlet water) provided information on the processes that affect the fate of As and other inorganic contaminants and their transfer towards surrounding environmental compartments (Thouin et al., 2017). After Zn, As was the most mobile inorganic contaminant in the soil water, with concentrations ranging from 20 to 110 µM. The present study was focused on the evolution of the solid compartment: mineral phases and arsenic-associated microbial parameters. The goal work was to analyze changes in mineral phases and variations in arsenic-associated microbial parameters to increase our understanding of the As cycle in this highly-polluted material that is undergoing environmental exposure.

2. Materials and methods

Experiment and soil sampling

Soil was collected at the site named "Place-à-Gaz" (Spincourt Forest, 20 km from Verdun, France) and characterized by Bausinger et al. (2007) and Thouin et al. (2016). It contains slag, coal ash, and residues from ammunition resulting in high concentrations of Zn, As, Cu, and Pb and high organic content (25.9 %).

All soil samples described here come from the instrumented mesocosm experiment presented in Thouin et al. (2017) and shown in supplementary material (SM1). Water and solute fluxes of polluted soil were monitored for 276 days using the experimental device, which consisted of a closed stainless steel column (1 m in diameter and 120 cm high), filled with 610 kg of homogenized contaminated soil. After three months of stabilization, the soil was subjected to dry/wet cycles (over a period of about eight (8) months) and to the addition of organic forest litter at the top of the surface soil at the midpoint of the experiment (after four (4) months at T4)(Fig.1.a). The dry period was characterized by a saturation limited to the mesocosm bottom, and by the addition of around 12 L of Mont Roucous mineral water once a week. The wet period was characterized by the elevation of the water level and by the addition of 6 L of water every two days. Rainfall was simulated by a sprinkler system. In order to obtain the data previously presented in Thouin et al. (2017), soil solution was sampled at four sampling levels (H1, H2, H3 and H4; Fig.1.a) thanks to inert porous probes. H1 and H2 levels were permanently unsaturated, H4 level was permanently saturated and H3 level was not saturated during dry periods but was saturated during wet periods.

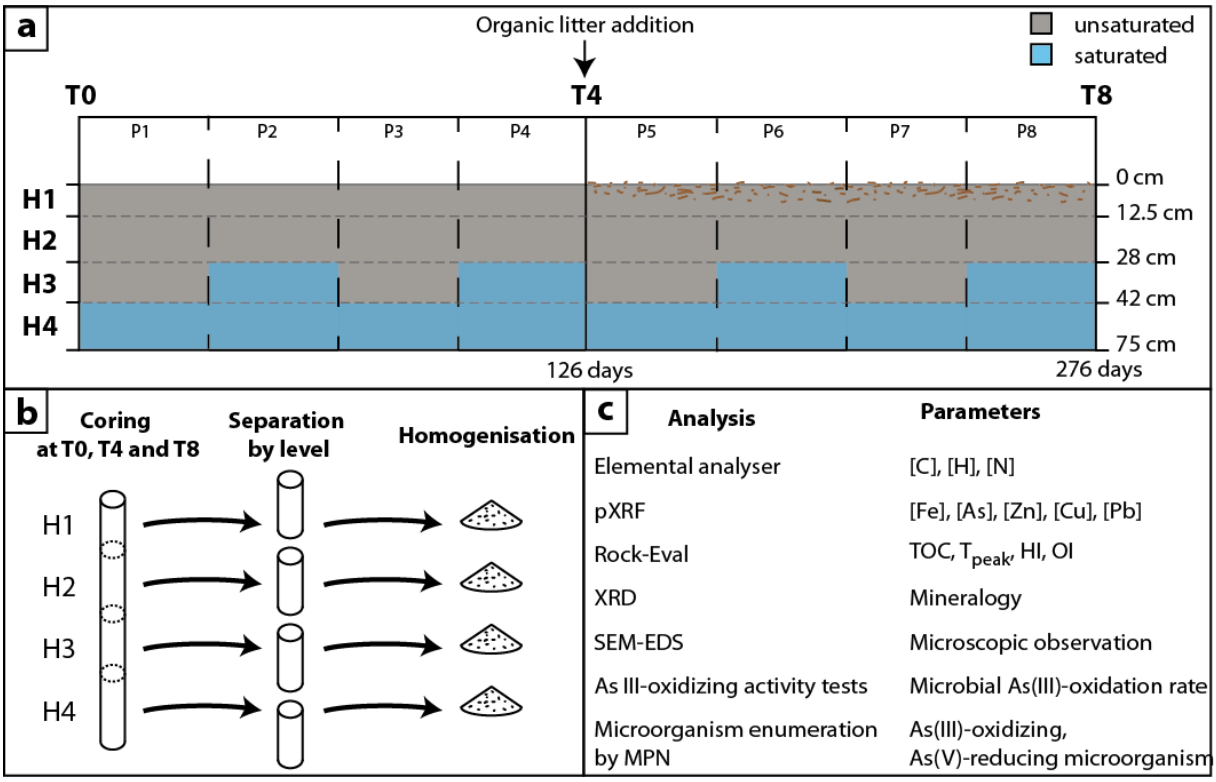


Fig.1. a. Experiment design. P1, P3, P5, P7 and P2, P4, P6, P8 were respectively dry and wet periods. From the beginning of P5 forest litter was added at the top of the contaminated soil. H4 was permanently saturated; H2 and H1 were never saturated. The H3 level was not saturated in the dry periods and saturated in the wet periods (modified from Thouin *et al.*,, 2017). b. Coring and sampling of solid material at T0 (at the beginning of the experiment), T4 (after 4 months just before the addition of organic litter) and T8 (at the end of this experiment, i.e. after 8 months). c. Analytical methods and associated parameters performed on each soil sample.

Coring was performed in the mesocosm using 5 cm diameter stainless steel pipes, at three steps of the experiment: at the beginning (T0), before the addition of fragmented forest litter at the end of month 4 (T4), and at the end of month 8 (T8). After sampling, the pipes were clogged and put back in place in the soil to fill the empty space. Each core was separated into four samples, H1 at a depth of 0-12.5 cm, H2 at 12.5-28 cm, H3 at 28-42 cm, and H4 at 42-75 cm, corresponding to the soil water sampling levels (Fig.1.b). These samples were homogenised and collected in sterile glass jars that were tightly closed and stored at 5°C.

Analytical techniques

For chemical analyses, soil samples were dried and ground to 70 µm. Total carbon, nitrogen, and hydrogen were quantified in powdered samples, using an elemental flash pyrolyser analyser (Flash 2000, Thermo Fischer Scientific). Total organic carbon (TOC), hydrogen index (HI), oxygen index (OI), and maximum temperature of pyrolysable OM (T_{peak}) were determined by Rock-Eval pyrolysis (Rock-Eval 6 Turbo, Vinci Technologies). The operating principles of this apparatus are described in Lafargue et al. (1998). HI can be used as a maturation

indicator and is calculated from the amounts of hydrocarbons generated through thermal cracking of nonvolatile organic matter relative to the amount of organic carbon. OI represents the amount of hydrogen relative to the amount of organic carbon present in a sample. It is calculated from the amount of CO_2 and CO released during pyrolysis of the sample. T_{peak} is the accurate temperature experienced by the sample when producing the maximum amount of hydrocarbons. Total concentrations of As, Cu, Zn, Pb, and Fe were determined using an XL3t800 NITON© portable X-ray fluorescence field apparatus (pXRF). The correct correlation of the metal concentrations determined by this technique and by ICP-MS was previously checked in the same soil (Thouin et al., 2016).

The mineralogical composition of the bulk samples was determined by powder X-ray diffraction (XRD). XRD patterns were recorded using an INEL CPS120 diffractometer montage transmission (Debye-Scherrer geometry) equipped with a Co anode (Co $K\alpha_1$ = 1.78897 Å) and operating at 35 kV and 35 mA. Scans were recorded from 5° to 90° (2θ) with angular steps of 0.03° and a total acquisition time of 210 min.

Scanning electron microscopy (SEM) and energy dispersive X-ray spectroscopy (EDS) were used to study the structural evolution of As and metal carrier phases during the experiment and to identify possible new precipitated phases. The samples were air dried, deposited on a carbon adhesive and directly analyzed. All types of grains were investigated for morphological observation and elemental distribution. SEM was performed on a TM 3000 (Hitachi) operating at 15 kV accelerating voltage. The SEM was coupled to a Swift ED 3000 X-Stream module (Hitachi). The acquisition time of EDS point analyses was 300 seconds.

As(III)-oxidizing activity tests and bacterial enumeration

Soil samples were incubated at 25°C for 72 h before starting the As(III)-oxidizing activity tests and the enumeration of As(III)-oxidizing and As(V)-reducing microorganisms. It was previously shown that this step allows restoring As-related microbial activities in soil and sediment samples that were stored at 5°C (Lescure et al., 2013; 2016). The As(III)-oxidizing tests were performed in triplicate in 250 mL Erlenmeyer flasks filled with 100 mL of CAsO1 medium (Bachate et al., 2002) supplemented with 1 mM As(III) and inoculated with a mass of material equivalent to 0.2 g of dry weight. Flasks were plugged with cotton to retain oxidizing conditions and were incubated at 25° under agitation (100 rpm). Samples were filtrated (0.45 µm) and stored at -20°C until analysis. As(III) and As(V) were separated using the PDC/MIBK method (Battaglia-Brunet et al., 2002). Separated neutral fraction, attributed to As(V) was then quantified by Flame Atomic Absorption Spectrometry (FAAS) (Varian, Palo

Alto, CA, USA). As(III)-oxidizing rates were determined by linear regression fitting of the As(V) concentration versus time line, during the reaction.

The evolution of the concentration in As(III)-oxidizing and As(V)-reducing microorganisms was followed using the Most Probable Number method (MPN). The method for As(III)-oxidizing microorganisms is detailed in Thouin et al. (2016). For As(V)-reducing microorganisms (method adapted from Kuai et al., 2001), fresh soil (equivalent to 0.2 g dry soil) was placed in a sterile, glass Erlenmeyer flask with 10 mL of sterile physiological saline (9 $g.L^{-1}$ NaCl in demineralized water), shaken for 30 min at 25°C, then sonicated 2 x 20 s at 45 kHz. Triplicate suspensions were prepared for each sample. Soil suspensions were diluted in sterile physiological saline solution to a dilution of 10^{-6}. CAsO1 basal mineral medium (Battaglia-Brunet et al., 2002) was complemented with 20 mM lactic acid and As(V) (100 $mg.L^{-1}$). The medium was distributed over Microtest TM Tissue culture plates (96 wells), 250 µL per well. Each well was inoculated with 25 µL of diluted soil suspension. Five wells were inoculated with each dilution. Culture plates were incubated at 25°C for 10 days in anaerobic jars with Anaerocult packs (Merck). The presence of As(III) formed in the wells during incubation was revealed by the formation of As(III)-PyrrolidineDithioCarbamate (PDC), an insoluble white complex: 80 µL of 0.1 M acetate buffer (pH 5) and 40 µL PDC solution (5 $g.L^{-1}$) were added to each well. The number of positive wells for each dilution was determined, and the most probable number of As(V)-reducing microorganisms was given by the Mc Grady table for five tubes.

Statistical analyses

Statistical tests were carried out using R 3.2.4 (www.r-project.org). Pearson correlations were calculated with the four soil samples at three time steps *i.e.* 12 observations. Principal component analysis (PCA) was performed on biogeochemical parameters on the same observations.

3. Results and discussion

3.1. Stability of As bearing mineral phases

Relationship between As and metals

As and metal concentrations measured/quantified by the pXRF method were high in all soil samples, in the following decreasing order As > Fe > Zn > Cu > Pb (SM2). Arsenic concentrations ranged from 102,380 to 150,360 $mg.kg^{-1}$, Zn concentrations from 70,040 to 107,400 $mg.kg^{-1}$, Cu concentrations from 13,450 to 20,790 $mg.kg^{-1}$, and Pb concentrations from 3,490 to 6,030 $mg.kg^{-1}$ (SM2). These inorganic contaminant concentrations were very elevated and in the same range as those measured in other soil samples from the same site (Bausinger et al., 2007;

Thouin et al., 2016). Concentration variations were difficult to detect with depth and time because of the high heterogeneity of the soil. However, at the end of the experiment (T8), metal(loid) concentrations seemed to be distributed in a pattern showing higher values at the bottom of the mesocosm (H4) (Fig.2; SM2). Moreover, As and metals were less concentrated at the surface after eight (8) months than at the beginning of the experiment (Fig.2; SM2). These observations may be the result of the downward vertical transport of metals within the mesocosm and their accumulation in the saturated soil. Monitoring of metal(oid) concentrations in interstitial water (Thouin et al., 2017) showed that As was immobilized in the bottom level H4 of the mesocosm as its concentration values decreased from 60-80 µM in unsaturated soil to 40 µM in the saturated zone. However, this phenomenon was not observed with other inorganic contaminants. Moreover, the amounts of As released from the liquid phase in the saturated parts are too low to explain the increase of about 40,000 $mg.kg^{-1}$ at the bottom of the mesocosm. It seems more likely that these results highlight the downward particular transport of contaminant-bearing fine particles during the experiment, even if these results are not sufficient to confirm this hypothesis.

Arsenic concentration was significantly correlated with that of metals, as shown by Pearson indices > 0.80 (Fig.2), with the exception of Fe concentration which was not correlated with any other metal(loid)s. These results suggest that As, Zn, Cu, and Pb were mainly linked to the same solid phase, as shown in previous characterizations of the polluted material (Thouin et al., 2016), indicating that the principal As carrier was an amorphous phase containing high concentrations of metals.

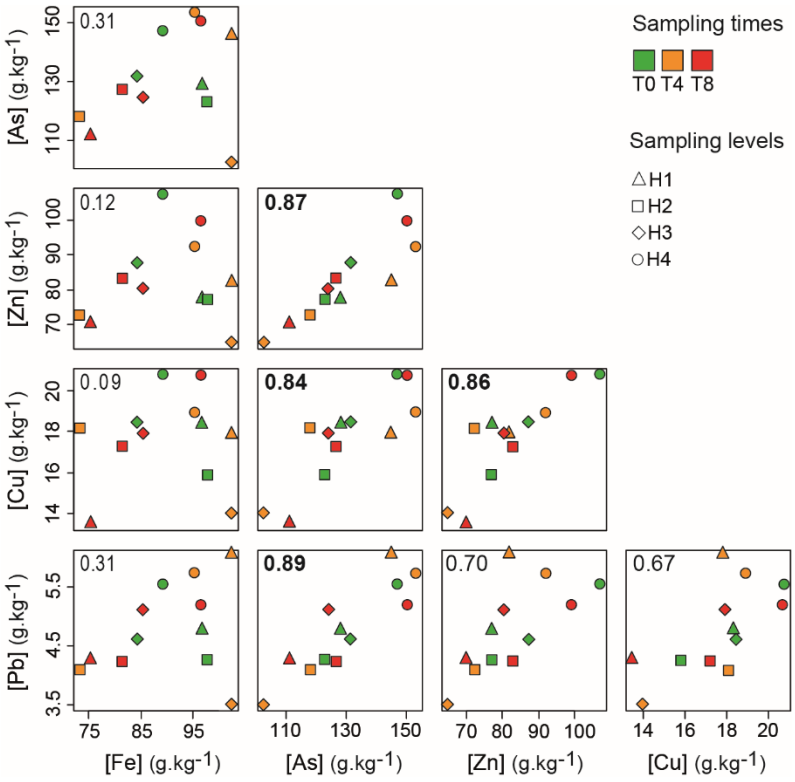


Fig.2. Scatterplot matrix of metal(loid) concentration. Pearson correlation coefficient of variables is specified in the upper-left corner of each panel (highest correlations are indicated in bold characters).

Stability of amorphous phases

Morphological evolution of amorphous phases was observed by SEM in various samples, so as to compare their stability at different times and under different environmental conditions. In the unsaturated levels, amorphous phases did not show evidence of weathering all along the experiment. Figure 2 shows the textural evolution of the vitrified amorphous phases in the soil level that was permanently water saturated. At the beginning of the experiment (Fig.3 (a)), this phase was characterized by a smooth texture with micro-cracks, similar to the morphology previously observed in samples from the site and attributed to the thermal process used to destroy the weapons (Thouin et al., 2016). After four (4) months of the mesocosm experiment, the surface of the amorphous phases had changed and taken on a rough texture (Fig.3 (b)). Edges of the cracks were altered and new fissure networks grew from the previous micro-cracks. At the end of the experiment, after 276 days of water saturation, the fissure networks covered the entire surface of the amorphous phases, which had become highly irregular (Fig.3 (c)). Similar observations have been made during the alteration of a partially vitrified metallurgical waste (Seignez et al., 2007). This morphological evolution may be consistent with dissolution of amorphous phase surfaces in the saturated soil, which should be accompanied by the release of As, Zn, Cu, Pb. However, metal(oid)s behaved

differently with high As and Zn concentrations in solution, whereas Cu, Pb and Fe were not very mobile (Thouin et al., 2017).

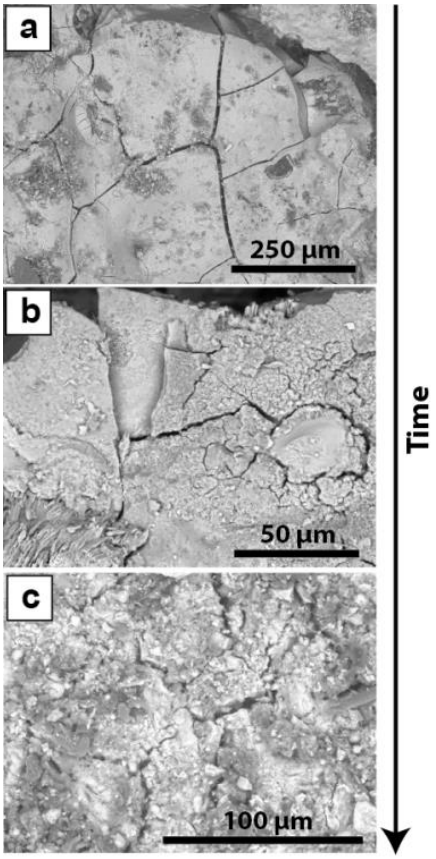


Fig.3. Backscattered electron images of amorphous phases in the saturated soil. (a), (b) and (c) illustration of three amorphous phases sampled in the H4 level at T0, T4 and T8 respectively.

Elemental composition of altered amorphous phases was investigated using SEM-EDS analyses (SM3). The elemental maps of Fe, Zn, As, Pb and Cu on amorphous phases presenting a partially altered surface showed a different distribution between Fe and Zn. In this study zone Fe content was lower in the smooth amorphous phases than in the rough surface. An alteration study of partially vitrified metallurgical waste composed primarily of an iron-silica-lime glass matrix showed that altered glass is characterized by relative enrichments of iron induced by high calcium depletion (Seignez et al., 2007). Here the results were similar, with higher iron concentrations in altered material even though this amorphous material does not have the same chemical composition (no silicium). Other studies showed that under oxidizing conditions, iron mobilized during dissolution of the vitrified material precipitated on the surface of the altered zone (Deneele 2002; Ettler et al., 2004). Our results can be explained by the precipitation of amorphous and poorly crystallized ferric oxides and/or hydrous ferric oxides (HFO) in the proximity of the amorphous phase, which can bind a portion of As and metals. This hypothesis is consistent with the low concentrations of mobile Fe (< 40 µM throughout the experiment, Thouin et al., 2017). The precipitation

of iron oxy-hydroxide permits the sorption of Cu and Pb (Swallow et al., 1980) and may also explain the low mobility of these elements. Moreover, the high adsorption of As(V) by amorphous HFO is a well-known phenomenon (Dixit and Hering 2003). Thus, precipitation of HFO resulting from the dissolution of amorphous phases in the water-saturated material may be one of the phenomena inducing the immobilization of As(V) that was observed in this specific environment of the mesocosm. The Zn depletion observed in the surface of the altered zone (SM3) seems to show the easier mobilization and the low affinity to HFO of Zn. These assumptions are consistent with the important Zn concentration in the soil solution, induced by favorable pH conditions (pH range of 5-6; Thouin et al., 2017), during the experiment.

Evolution of the mineralogical association

XRD analysis of soil samples from different depths was used to investigate the mineralogical evolution of the polluted material during the experiment (Fig.4). First, the high background of X-ray diffractograms confirmed the abundance of amorphous phases in the soil. Quartz and potassium and sodium feldspars were identified in each sample with a relative peak intensity that evolved slightly over time and depth. These silicates, which had already been observed in samples from the polluted site (Thouin et al., 2016), were attributed to the substrate, *i.e.* the clayey Woëvre formation.

Magnetite (Fe_3O_4) and franklinite ($ZnFe_2O_4$) were detected in most samples. Magnetite and franklinite exhibit a spinel structure with similar lattice parameters that result in an overlapping of their corresponding XRD peaks, so it is difficult to ascertain the presence of franklinite with XRD spectra. However, the Zn concentration in solids and the common occurrence of the magnetite-franklinite mineral association in metallurgical furnace wastes (Pisciella et al., 2001; Juillot et al., 2003; Dutra et al., 2006; Puziewicz et al., 2007; Seignez et al., 2007; Vereš 2014) and in vitrified products of electrostatic precipitator ash from municipal solid wastes (Le Forestier and Libourel 2008) suggest that magnetite-franklinite solid solutions are present as a result of the thermal destruction process. The presence of zincite in site soil samples (Thouin et al., 2016) and in metallurgical wastes, together with magnetite and franklinite (Dutra et al., 2006; Puziewicz et al., 2007; Vereš 2014), confirm the inherited character of these minerals in this context. Although not detected by XRD in the mesocosm samples, zincite, as well as magnetite and franklinite, were most probably present but in insufficient amounts for appropriate detection due to soil heterogeneity. No significant effect of dry/wet cycles or the addition of OM on the stability of these Fe and Zn minerals was detected.

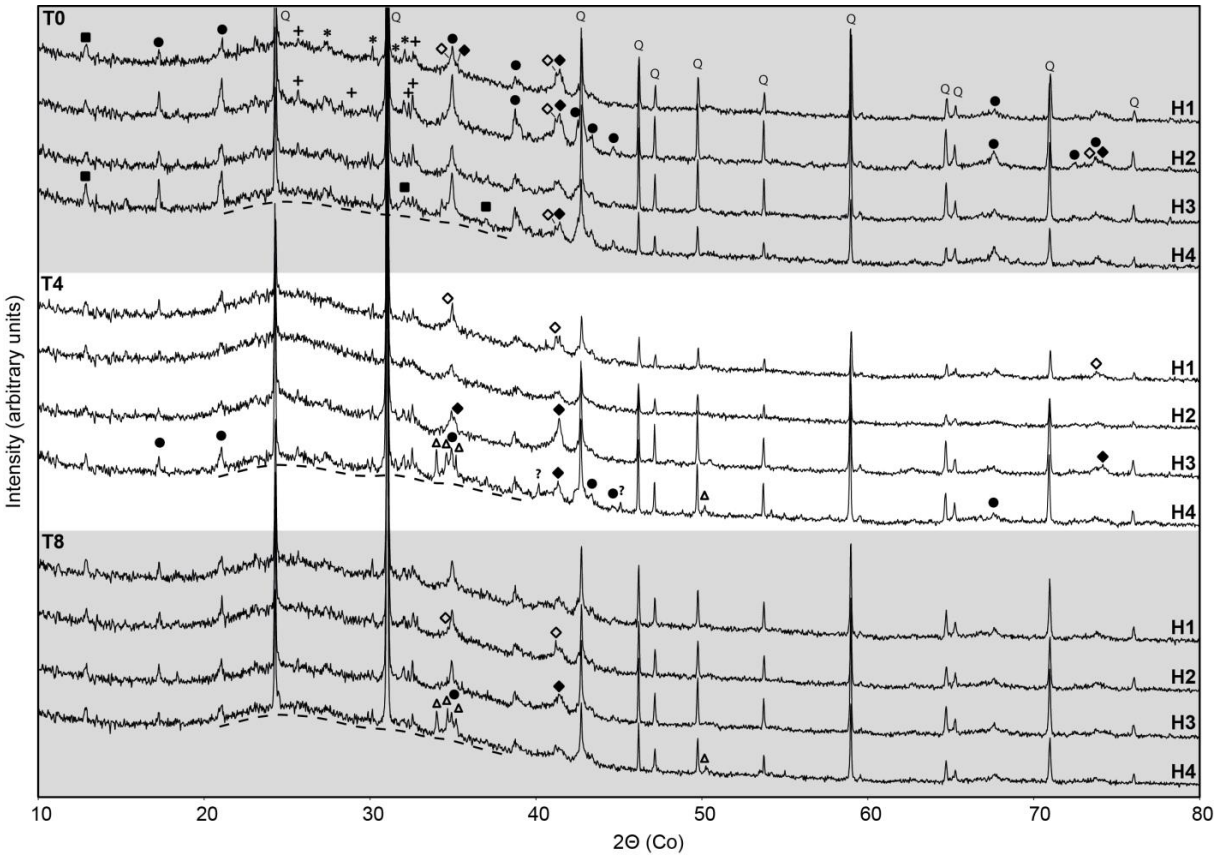


Fig.4. X-ray diffractograms of bulk soil samples. Q: quartz (ICDD-1045); ✱: sodium feldspar (ICDD 19-1184); ✚: potassium feldspar (ICDD 31-0966); ●:adamite (ICDD 39-1354); ■: Na-Pharmacosiderite (ICDD 38-0388); ◆: magnetite (ICDD 19-0629); ◇: franklinite (ICDD 22-1012); Δ: mimetite (ICDD 19-0683); and ?: unidentified mineral.

The Zn, Cu, and Fe arsenates previously observed in this soil (Thouin et al., 2016), adamite ($Zn_2AsO_4(OH)$), olivenite ($Cu_2AsO_4(OH)$), and pharmacosiderite ($(K,Na,Ba)Fe_4(AsO_4)_3(OH)_5\ 5H_2O$) were again identified in all samples (Fig.4). Adamite and olivenite are characterized by the same structure so they have similar XRD patterns, but SEM-EDS showed that crystals were mostly a solid solution of adamite and olivenite (SM4.a). Indeed, adamite-olivenite crystals were easily recognized because of their prismatic and acicular texture, and the ability to form large crystals that may grow on grain surfaces. Pharmacosiderite with a cubic structure was also observed (SM4.b). No evidence of weathering was observed on these arsenate minerals, which were present all along the soil profile.

Mimetite ($Pb_5(AsO_4)_3Cl$), a lead arsenate chloride, was detected exclusively in the water-saturated H4 level at T4 and T8 (Fig.4). Mimetite precipitation was proposed to be part of a soil treatment technology allowing the removal of arsenate ions from solution (Twidwell et al., 1994 ; Bajda et al., 2006). Indeed, mimetite precipitates under conditions of low Pb and arsenate concentrations and has a stability domain that covers the pH range of natural

waters (Magalhães and Silva 2003; Bajda 2010). Arsenate and chloride ions, which were present in high concentrations in interstitial water throughout the experiment, and the pH range of 5.5-6.0 (Thouin et al., 2017) were optimal for mimetite precipitation. The factor that limited mimetite precipitation in the soil was the low amount of dissolved Pb concentration. Mimetite precipitation in the saturated part of the soil means that Pb was previously released into solution under these conditions; this confirms the hypothesis of progressive dissolution of metal-bearing amorphous phases throughout the experiment. Mimetite was not observed with SEM, but micrometric grains with high lead and other metal concentrations were observed in the saturated depth level (SM4.c). This observation confirms that lead was released and then re-precipitated. Mimetite precipitation, promoted by soil water saturation, was probably one of the phenomena that caused the previously observed immobilization of Pb and As(V). Due to mimetite's broad pH stability range (down to pH = 2), this mineral represents a durable trap for As and Pb. However, the very low dissolved Pb concentration limited mimetite precipitation and relatively high amounts of As remained in solution.

3.2. Modification of the soil organic matter

Characterization of soil OM present in the mesocosm was performed using an elemental flash pyrolyser analyser and Rock-Eval pyrolysis. Results are represented in table 1. Total carbon (C) ranged from 14.7 to 27.8 %, and total hydrogen from 1.6 to 2.4 % in the mesocosm soil. The N content of soil ranged from 0.3 to 0.8 %. TOC ranged between 14.1 and 25.3 %. HI results were low for all mesocosm samples (< 0.18 mg HC. g^{-1} TOC) except for sample H1 – T8. The proportion of O containing OM (OI) ranged between 125 and 200 mg O_2. g^{-1} TOC. All T_{peak} values were higher than 440 °C, and were higher than 500 °C for two samples (H3 – T4 and H4 – T8). The high organic carbon content together with the HI and OI values are quite different from those expected in soil OM (Disnar et al., 2003), but instead show chemical signatures of charcoals (Wolf et al., 2013; Saenger et al., 2015).

Previous studies suggest that physical and chemical charcoal properties depend on the temperature of the fire (Schneider et al., 2010; Wolf et al., 2013). Charcoal formation begins with the loss of easily oxidizable OM (such as aliphatic and carboxylic compounds), thus with increasing temperature organic compounds progressively aromatize. High temperature combustion (> 700°C) may cause complete carbonization of OM and may form polyaromatic crystallites or graphite-like structures (Keiluweit et al., 2010). This restructuring of OM is expressed by an increase in TOC and a decrease in OI and HI. Wolf et al., (2013) studied the relationship between charcoal signatures and burning conditions. According to their data, our OM signature (HI/OI, T_{peak}) would correspond to a fire temperature ranging between 300 and 400 °C. However, this temperature seems to be relatively low for

melting metals (Fe, Cu, Zn, Pb) from shell parts, thus to form the amorphous phases. Wood was placed on top of the shell dumps during destruction. The temperature was probably higher in the center of the fire, thus explaining the difference between the fire temperature signal of charcoal and the total range of temperatures reached during combustion.

Table 1 Parameters related to OM

	Time	C[a]	H[a]	N[a]	C/N[a]	TOC[b]	T_{peak}[b]	HI[b]	OI[b]	HI/OI[b]
		%	%	%		%	°C	mg HC. g^{-1} TOC	mg O_2. g^{-1} TOC	
H1	T0	21.1	1.8	0.6	36.3	16.1	441	13	161	0.08
H2		23.8	2.1	0.7	36.2	24.9	446	11	125	0.09
H3		25.9	2.3	0.7	36.6	18.5	443	17	161	0.11
H4		27.8	2.4	0.8	37.0	14.6	445	15	200	0.08
H1	T4	27.1	2.4	0.7	38.1	15.3	446	15	184	0.08
H2		25.9	2.2	0.6	40.5	18.3	452	16	147	0.11
H3		14.7	1.5	0.3	53.5	14.1	542	18	157	0.11
H4		15.1	1.6	0.3	45.8	19.4	440	14	147	0.10
H1	T8	27.8	2.4	0.8	37.0	25.3	439	37	169	0.22
H2		22.6	1.8	0.4	53.2	23.2	445	16	151	0.11
H3		22.8	1.7	0.5	49.5	22.8	446	18	150	0.12
H4		17.1	1.6	0.4	46.2	17.5	559	18	154	0.12
Litter		38.5	4.7	1.8	21.4	30.5	369	268	205	1.31

a : Flash pyrolyser analyser; b : Rock-Eval 6

The forest litter added at T4 had a very different signal from that of the soil. It has higher organic carbon (30.5 %) and nitrogen (1.8 %) concentrations, higher HI (268 mg HC. g^{-1} TOC) and OI (205 mg O_2. g^{-1} TOC) values, and a lower T_{peak} (369 °C). Disnar et al. (2003) determined that fresh or fragmented litter normally has high TOC values (10-40%) and HI values higher than 300 mg HC. g^{-1} TOC. The T_{peak} of 360-370 °C is mostly attributed to cellulose and/or lignin, two major components of woody tissues frequently observed in litters. These results confirmed the immature nature of the organic litter added to the top soil of the mesocosm.

The intrinsic OM of the "Place-à-Gaz" soil, with a high C/N and low HI/OI ratio has characteristics of a barely biodegradable material (Tab.1 and SM5). However, the addition of fragmented forest litter enhanced the proportion of biodegradable OM in the top soil. The effect of forest litter was visible on surface soil sample H1 – T8, which had a higher organic carbon content (25.3 %) and a higher HI/OI ratio (0.22; Tab.1 and SM5), but not a higher

C/N ratio. Addition of organic litter increased the carbon mineralization rate in the mesocosm (Thouin et al., 2017), as a result, it was supposed that the addition of litter increased microbial activity.

3.3. Biogeochemistry of arsenic

Microbial arsenic transformation

As(III)-oxidizing activity tests were used to evaluate the potential for microbial As(III) oxidation during the experiment (Fig. 5). These global activity tests integrate the diversity and abundance of microflora and environmental soil conditions (Lescure et al., 2016). With samples collected at T0, As(III) oxidation started after 70 and 90 hours of lapsed time at all levels. The results of microbial As(III) oxidation activity tests at T0 were consistent with results previously obtained with soil sampled from the most polluted zone of the "Place-à-Gaz" site (Thouin et al., 2016), with identical latency of about 100 h. Here, the lapsed time decreased progressively during the mesocosm experiment, particularly in the water-saturated levels. At T8, the As(III) oxidation kinetics of each sample were well separated temporally, with complete As(III) oxidation achieved in time periods that increased as follows: H4 < H3 < H2 < H1. The rate of microbial As(III) oxidation was consistently higher in saturated or alternatively saturated/unsaturated levels H4 and H3 than in unsaturated levels H1 and H2 (except for H3 T0) (Fig.5.b). The rate of microbial As(III) oxidation decreased over time, mostly in H1 and H4, whose As(V) values decrease from 1.3 and 2.2 mg of As(V).$mL^{-1}.h^{-1}$ at T0 to 0.8 and 1.3 mg of As(V).$mL^{-1}.h^{-1}$ at T8.

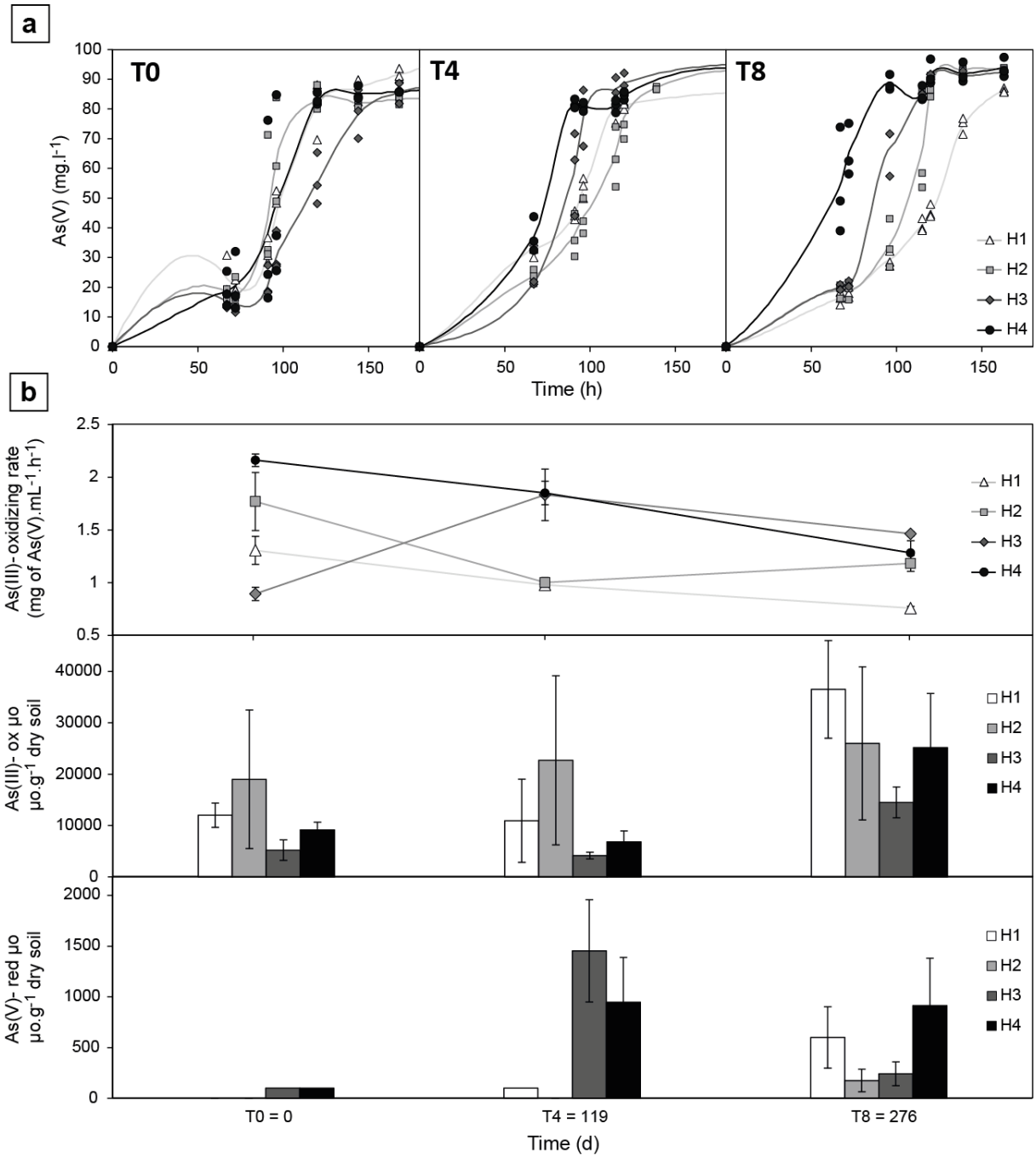


Fig.5. Microbial As(III)-oxidizing and As(V)-reducing activities. a: Evolution of As(V) concentration during the As(III)-oxidizing activity test for the four soil samples at T0, T4 and T8. b: Plot of As(III) oxidation rates corresponding to the activity tests in "a". Concentration of As(III)-oxidizing and As(V)-reducing microorganisms evaluated by MPN. Errors bars represent the standard deviation of the mean of three replicates for the four soil samples. For As(V)-reducing microorganisms a lack of value means that results from the two or three replicates were < 50 µo.g^{-1} dry soil. (ox: oxidizing; red: reducing; µo: microorganisms).

The evolution of abundance of As(III)-oxidizing and As(V)-reducing microorganisms was followed by MPN (Fig.5.b). Between T0 and T4, As(III)-oxidizing microorganism concentrations were stable with higher values in H2 and lower in H3.

After the addition of fragmented forest litter, the concentration of As(III)-oxidizing microorganisms increased in all levels, and particularly in H1. As(V)-reducing microorganisms abundance that could be estimated by the selected MPN method were significantly lower than As(III)-oxidizing microorganisms (one order of magnitude less). At T0, less than 100 As(V)-reducing microorganisms per gram of dry soil were observed. After four (4) months of the experiment, As(V)-reducing microorganism concentrations increased in the saturated and alternatively saturated/unsaturated levels. At T8, the concentration of As(V)-reducing microorganisms increased in H1 and H2, decreased in H3, and remained constant in H4. Thus, both water saturation (for H3 and H4) and OM supply (for H1 and H2) seemed to promote the growth of As(V)-reducing micro-organisms.

Effect of water saturation and addition of litter on arsenic biogeochemical cycle

The impact of water saturation levels and redox oscillation on As solubility has been described in many studies (Kumpiene et al., 2009 ; Weber et al., 2010 ; Parsons et al., 2013 ; Couture et al., 2015) where it was shown that soil saturation increased As solubility by the way of reduction of Fe oxides together with more efficient microbial reduction of As(V). Increased As(III) concentration in soil solution previously observed in the saturated level H4 of the mesocosm (Thouin et al., 2017) could be related to increased As(V)-reducing microorganism concentrations in the saturated zones. The stimulation of microbial As(V)-reducing activity induced by soil saturation may have negatively impacted the overall As(III) oxidation rate in water-saturated levels, but could not explain a decreased As(III) oxidation rate in unsaturated levels H1 and H2 (Fig.5.a T8).

OM may also affect microbial As(III) oxidizing activity. For example, high concentrations of organic substrates may inhibit this activity (Challan-Belval et al., 2009 ; Bachate et al., 2012 ; Lescure et al., 2016) and may also stimulate aerobic As(V)-reducing activity of soil microorganisms (Yamamura et al., 2009). The As(III) oxidation rate results from the overall activity of all microorganisms involved in As speciation, because microbial As(III) oxidation and As(V) reduction can occur simultaneously, even under aerobic conditions.

To describe more precisely the impact of the addition of litter on the available microbial parameters, a principal components analysis (PCA) was built (Fig.6), including variables that describe OM quantities and qualities (TOC, DOC, HI/OI, C/N), microbial As transformation parameters (As(III)-oxidation rate, concentrations of As(III)-oxidizing microorganisms and As(V)-reducing microorganisms), and the variables related to the water phase of the mesocosm, given in Thouin et al., (2017): As speciation and mobility in the interstitial water ([As], [As(III)], [As(V)]), and physicochemical parameters of water (pH, Eh).

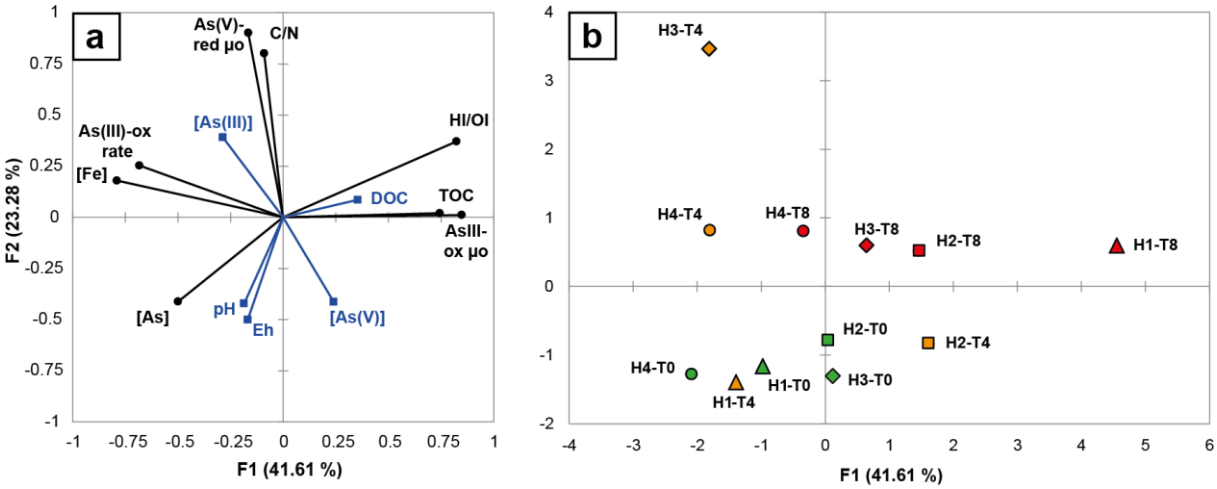


Fig.6. PCA using biogeochemical parameters of soil samples (black) with geochemical parameters of soil solutions (from Thouin *et al.*,, 2017) as supplementary data (blue). a: Correlation circle showing variable relationships. b: Factorial plan showing samples. (ox: oxidizing; red: reducing; µo: microorganisms). Pearson correlation matrix was presented in SM6.

As previously observed, the As(III) oxidation rate seems to be negatively correlated with As(III)-oxidizing microorganism concentrations (p = -0.50) and with DOC (p = -0.53) and HI/OI (p = -0.50) (Fig.6.a). This distribution was brought by principal component F1, which represented about 40% of total variability. For this component, the surface soil (H1-T8), as the end member, is pulled to the right (Fig.6.b) due to the combined effect of DOC, TOC, HI/OI, and As(III)-oxidizing microorganism concentrations. This level was the most impacted by the addition of forest litter. The sample distribution along the principal component F1 shows the overall effect of the litter on the entire mesocosm, with an enhanced influence towards the right from T4 to T8. Moreover, the distribution of T8 samples clearly depends on their depth because, as previously discussed, the deeper level was less impacted by the addition of OM.

Principal component F2 accounts for 23% of total variability. The concentration of As(V)-reducing microorganisms and the C/N ratio were correlated (p = 0.59) and were the primary contributors to F2. The previously mentioned positive effect of soil saturation on As(V)-reducing microorganisms is expressed by the upward translation of samples H3 and H4 between T0 and T4 along the F2 axis (Fig.6.b). Bioavailable OM may stimulate the As(V)-reducing activity of soil microorganisms under aerobic conditions (Yamamura et al., 2009) because the As(V)-reducing mechanism linked to the As resistance system consumes energy. In our study, concentrations of As(V)-reducing microorganisms increased in the non-saturated soil after the addition of fragmented litter. However, As(V)-reducing microorganisms were correlated to the C/N ratio (p = 0.59) but were not correlated to total OM concentrations (TOC, p = -0.18; DOC, p = -0.09). The relationship between As(V)-

reducing microorganism concentrations in the soil and OM qualities and quantities cannot be confirmed here. Finally, the quantity of As(V)-reducing microorganisms was correlated with As(III) concentrations in soil interstitial water ($p = 0.76$) suggesting that microbial As-reducing activity was promoted by soil saturation. However, the overall proportion of As(III) in interstitial water remained lower that of As(V) (10 to 20%, Thouin et al., 2017).

The present experiment differs from previous studies by two main aspects: (1) the extreme level of metals and As concentrations, that resemble those found in mining wastes (Drewniak et al., 2008) but without the high concentration in sulfur species, and (2) the fact that in spite of water saturation and addition or OM, the redox potential did not reach very low values. Weber et al. (2010) observed a decrease of redox potential down to 0 mV in the porewater of their contaminated surface soil after 20 days of flooding with artificial river water, with a simultaneous strong reduction of As(V), whereas in our experiment, the redox potential always remained higher than +100 mV (Thouin et al., 2017). As a fact, most of the reported studies about redox dynamic were performed with soils or sediments less contaminated than the "Place-à-Gaz" material: 300 ppm As in a polluted floodplain soil (Weber *et al.*, 2010), 375 ppm As in an artificially polluted soil (Couture et al., 2015), 63 ppm As in a contaminated sediment (Moon et al., 2017) compared with 100 000 ppm As in our soil. Thus, the present experiment provides information about microbial As transformation in a biogeochemical environment that was not previously explored in variable redox conditions. Thouin et al. (2016) found that elevated toxic element concentrations (Cu, Pb, Zn, As) seemed to have exerted a selective pressure on the microbial communities, with higher As(III)-oxidizing rates and lower microbial activity involved in carbon mineralization of the microbial populations from the most polluted zone of the site. Thus, phenomena linked to high concentrations of metals and arsenic may have attenuated the decrease of redox potential linked to oxygen consumption in the saturated level, while OM was provided, compared with less polluted environments. Up to now, all As(III)-oxidizing bacteria isolated from soils were heterotrophs or facultative autotrophs (Inskeep et al., 2007; Bachate et al., 2012; Bahar et al., 2013; Dong et al., 2014). The increasing amount of OM and its quality therefore promoted the growth of As(III)-oxidizing microorganisms. However, several studies have shown that elevated concentrations of bioavailable OM negatively impact As(III)-oxidizing bacterial activity (Challan-Belval et al., 2009; Bachate et al., 2012; Lescure et al., 2016). The opposite trend of overall As(III) oxidizing rate with increasing As(III)-oxidizing microorganisms concentration ($p = -0.50$) and with the quality and quantity of OM seems to confirm the inhibiting effect of OM on the specific activity of As(III)–oxidizing microbes. However, globally, As(III) oxidizing microorganisms remained active in presence of OM, even in the saturated zones of the mesocosm, in accordance

with the predominance of As(V) in the interstitial water all along the experiment and with the formation of mimetite. This original phenomenon could result from the particular balance between As and OM microbial transformations in the presence of extremely high concentrations of toxic contaminants.

4. Conclusion

The mesocosm experiment provided important information about the mineralogical evolution and stability of As and heavy metal mineral carriers present in the highly-polluted soil at the "Place-à-Gaz" site, as it underwent environmental changes. As, Cu, and Zn-bearing amorphous phases were altered under saturated conditions. Related to this alteration process, SEM results suggest a mechanism of dissolution and re-precipitation of iron in the form of amorphous oxides that may be a secondary sink for As and metals. In contrast, no traces of alteration were observed on crystallized arsenate minerals present in the soil at the beginning of the experiment. However, the formation of mimetite, a lead arsenate chloride mineral, was detected in water saturated zones. This phenomenon contributed to the immobilization of As(V) and Pb, but was limited by the low Pb concentration of the soil solution.

The input of OM contributed to the growth of both As(III)-oxidizing and As(V)-reducing microorganisms and negatively impacted the overall As(III) oxidation efficiency. This last phenomenon may be related to both the inhibition of microbial As(III)-oxidizing activities and the development of As(V)-reducing microorganisms. However, As(III)-oxidizing activity remained the major microbial-related phenomenon even in the saturated zones. Altogether, results from the mesocosm experiment show that water saturation of the "Place-à-Gaz" soil during high precipitation episodes is likely to promote the release of Zn and As into the water compartment. However, microbial As(III) oxidation activities, adsorption of As(V) on HFO and precipitation of mimetite are all processes observed during the experiment that contribute to partial immobilization of As, i.e. a decrease of total soluble As. The elucidation of these geochemical and biogeochemical processes at the mesocosm scale will contribute to more precise evaluations of the risks associated with these types of polluted sites and to better design management strategies.

Acknowledgments

This work was co-funded by the Région Centre Val-de-Loire and BRGM (convention 00087485) and the Labex Voltaire (ANR-10-LABX-100-01). The authors wish to thank Philippe Penhoud, Marielle Hatton, and Rachel Boscardin (ISTO) for XRD, CHNS and Rock-Eval results, Pascal Auger (BRGM) for Niton analyses, and Daniel Hube (BRGM) who introduced the environmental issue and provided the polluted material.

References

Bachate, S.P., Khapare, R.M., and Kodam, K.M. (2012). Oxidation of arsenite by two β-proteobacteria isolated from soil. Applied Microbiology and Biotechnology *93*, 2135–2145.
DOI: 10.1007/s00253-011-3606-7

Bahar, M.M., Megharaj, M., and Naidu, R. (2013). Kinetics of arsenite oxidation by Variovorax sp. MM-1 isolated from a soil and identification of arsenite oxidase gene. Journal of Hazardous Materials *262*, 997–1003.
DOI: 10.1016/j.jhazmat.2012.11.064

Bajda, T., Szmit, E., and Manecki, M. (2006). Removal of As (V) from solutions by precipitations of mimetite Pb5 (AsO4) 3Cl. Environmental Engineering, 119-124.

Bajda, T. (2010). Solubility of mimetite $Pb_5(AsO_4)_3Cl$ at 5–55°C. Environmental Chemistry *7*, 268.
DOI: 10.1071/EN10021

Battaglia-Brunet, F., Dictor, M.-C., Garrido, F., Crouzet, C., Morin, D., Dekeyser, K., Clarens, M., and Baranger, P. (2002). An arsenic(III)-oxidizing bacterial population: selection, characterization, and performance in reactors. Journal of Applied Microbiology *93*, 656–667.
DOI: 10.1046/j.1365-2672.2002.01726.x

Bausinger, T., and Preuβ, J. (2005). Environmental remnants of the First World War: Soil contamination of a burning ground for arsenical Ammunition. Bulletin of Environmental Contamination and Toxicology *74*, 1045–1053.
DOI: 10.1007/s00128-005-0686-z

Bausinger, T., Bonnaire, E., and Preuß, J. (2007). Exposure assessment of a burning ground for chemical ammunition on the Great War battlefields of Verdun. Science of The Total Environment *382*, 259–271.
DOI: 10.1016/j.scitotenv.2007.04.029

Challan-Belval, S., Garnier, F., Michel, C., Chautard, S., Breeze, D., and Garrido, F. (2009). Enhancing pozzolana colonization by As(III)-oxidizing bacteria for bioremediation purposes. Applied Microbiology and Biotechnology *84*, 565–573.
DOI: 10.1007/s00253-009-2077-6

Couture, R.-M., Charlet, L., Markelova, E., Madé, B., and Parsons, C.T. (2015). On–Off Mobilization of Contaminants in Soils during Redox Oscillations. Environmental Science & Technology. *49*, 3015–3023.
DOI: 10.1021/es5061879

Deneele, D (2002). Caractérisation, simulations expérimentales et thermodynamiques de l'altération de déchets vitreux: les scories de première fusion de plomb et de zinc, University Ph.D. Thesis, University of Lille 1, France, 2002, 198 pp.

Disnar, J.R., Guillet, B., Keravis, D., Di-Giovanni, C., and Sebag, D. (2003). Soil organic matter (SOM) characterization by Rock-Eval pyrolysis: scope and limitations. Organic Geochemistry *34*, 327–343.
DOI: 10.1016/S0146-6380(02)00239-5

Dixit, S., and Hering, J.G. (2003). Comparison of arsenic(V) and arsenic(III) sorption onto iron oxide minerals: implications for arsenic mobility. Environmental Science and Technology *37*, 4182–4189.
DOI: 10.1021/es030309t

Dong, D., Ohtsuka, T., Dong, D.T., and Amachi, S. (2014). Arsenite oxidation by a facultative chemolithoautotrophic *Sinorhizobium* sp. KGO-5 isolated from arsenic-contaminated soil. Bioscience, Biotechnology, and Biochemistry *78*, 1963–1970.

DOI: 10.1080/09168451.2014.940276

Drewniak, L., Matlakowska R., Sklodowska, A. (2008). Arsenite and Arsenate Metabolism of *Sinorhizobium* sp. M14 Living in the Extreme Environment of the Zloty Stok Gold Mine. Geomicrobiology Journal 25, 363–370.
DOI: 10.1080/01490450802402836

Drewniak, L., and Sklodowska, A. (2013). Arsenic-transforming microbes and their role in biomining processes. Environmental Science and Pollution Research*20*, 7728–7739.
DOI: 10.1007/s11356-012-1449-0

Dutra, A.J.B., Paiva, P.R.P., and Tavares, L.M. (2006). Alkaline leaching of zinc from electric arc furnace steel dust. Minerals Engineering *19*, 478–485.
DOI: 10.1016/j.mineng.2005.08.013

Ettler, V., Komárková, M., Jehlička, J., Coufal, P., Hradil, D., Machovič, V., and Delorme, F. (2004). Leaching of lead metallurgical slag in citric solutions implications for disposal and weathering in soil environments. Chemosphere *57*, 567–577.
DOI: 10.1016/j.chemosphere.2004.07.022

Inskeep, W. P., Macur, R. E., Hamamura, N. H., Warelow, T. P., Ward, S. A., Santini, J. M. (2007). Detection, diversity and expression of aerobic bacterial arsenite oxidase genes. Environmental Microbiology *9*, 934-943.
DOI: 10.1111/j.1462-2920.2006.01215.x

Moon, H. S., Kim, B. A., Hyun, S. Y., Lee Y.-H., Shin D. (2017). Effect of the redox dynamics on microbial-mediated As transformation coupled with Fe and S in flow-through sediment columns. Journal of Hazardous Materials *329*, 280-289.
DOI: 10.1016/j.jhazmat.2017.01.034

Juillot, F., Morin, G., Ildefonse, P., Trainor, T.P., Benedetti, M., Galoisy, L., Calas, G., and Brown, G.E. (2003). Occurrence of Zn/Al hydrotalcite in smelter-impacted soils from northern France: Evidence from EXAFS spectroscopy and chemical extractions. American Mineralogist *88*, 509–526.
DOI: 10.2138/am-2003-0405

Keiluweit, M., Nico, P.S., Johnson, M.G., and Kleber, M. (2010). Dynamic molecular structure of plant biomass-derived black carbon (biochar). Environmental Science & Technology *44*, 1247–1253.
DOI: 10.1021/es9031419

Kuai, L., Nair A. A., Polz M. F. (2001) Rapid and simple method for the Most-Probable-Number estimation of arsenic-reducing bacteria. Applied and Environmental Microbiology 67, 3168-3173.
DOI: 10.1128/AEM.67.7.3168-3173.2001

Kumpiene, J., Ragnvaldsson, D., Lövgren, L., Tesfalidet, S., Gustavsson, B., Lättström, A., Leffler, P., and Maurice, C. (2009). Impact of water saturation level on arsenic and metal mobility in the Fe-amended soil. Chemosphere *74*, 206–215.
DOI: 10.1016/j.chemosphere.2008.09.068

Lafargue, E., Marquis, F., and Pillot, D. (1998). Rock-Eval 6 Applications in Hydrocarbon Exploration, Production, and Soil Contamination Studies. Rev. Inst. Fr. Pét. *53*, 421–437.
DOI: 10.2516/ogst:1998036

Le Forestier, L., Libourel, G. (2008) High temperature behavior of electrostatic precipitator ash from municipal solid waste combustors. Journal of Hazardous Materials *154*, 373-380.
DOI: 10.1016/j.jhazmat.2007.10.034

Lescure T., Carpentier A., Battaglia-Brunet F., Morel-Desrosiers N.. (2013) Oxidation of As(III) by the Bacterial Community of a Marine Sediment Monitored by Microcalorimetry. Geomicrobiology Journal 30, 540-548.

DOI: 10.1080/01490451.2012.737088

Lescure, T., Moreau, J., Charles, C., Ben Ali Saanda, T., Thouin, H., Pillas, N., Bauda, P., Lamy, I., and Battaglia-Brunet, F. (2016). Influence of organic matters on AsIII oxidation by the microflora of polluted soils. Environmental Geochemistry and Health *38*, 911–925.
DOI: 10.1007/s10653-015-9771-3

Magalhães, M.C.F., and Silva, M.C.M. (2003). Stability of lead(II) arsenates. Monatshefte Für Chemie / Chemical Monthly *134*(5), 735–743.
DOI: 10.1007/s00706-002-0581-9

de Mello, J.W.V., Talbott, J.L., Scott, J., Roy, W.R., and Stucki, J.W. (2007). Arsenic speciation in arsenic-rich Brazilian soils from gold mining sites under anaerobic incubation. Environmental Science and Pollution Research - International *14*, 388–396.
DOI: 10.1065/espr2006.08.330

Parsons, C.T., Couture, R.-M., Omoregie, E.O., Bardelli, F., Greneche, J.-M., Roman-Ross, G., and Charlet, L. (2013). The impact of oscillating redox conditions: Arsenic immobilisation in contaminated calcareous floodplain soils. Environmental Pollution *178*, 254–263.
DOI : 10.1016/j.envpol.2013.02.028

Pisciella, P., Crisucci, S., Karamanov, A., and Pelino, M. (2001). Chemical durability of glasses obtained by vitrification of industrial wastes. Waste Management *21*, 1–9.
DOI: 10.1016/S0956-053X(00)00077-5

Puziewicz, J., Zainoun, K., and Bril, H. (2007). Primary phases in pyrometallurgical slags from a zinc-smelting waste dump, swietochlowice, upper silesia, poland. The Canadian Mineralogist *45*, 1189–1200.
DOI: 10.2113/gscanmin.45.5.1189

Saenger, A., Cécillon, L., Poulenard, J., Bureau, F., De Daniéli, S., Gonzalez, J.-M., and Brun, J.-J. (2015). Surveying the carbon pools of mountain soils: A comparison of physical fractionation and Rock-Eval pyrolysis. Geoderma *241–242*, 279–288.
DOI: 10.1016/j.geoderma.2014.12.001

Schneider, M.P.W., Hilf, M., Vogt, U.F., and Schmidt, M.W.I. (2010). The benzene polycarboxylic acid (BPCA) pattern of wood pyrolyzed between 200°C and 1000°C. Organic Geochemistry *41*, 1082–1088.
DOI: 10.1016/j.orggeochem.2010.07.001

Seignez, N., Gauthier, A., Bulteel, D., Buatier, M., Recourt, P., Damidot, D., and Potdevin, J.L. (2007). Effect of Pb-rich and Fe-rich entities during alteration of a partially vitrified metallurgical waste. Journal of Hazardous Materials *149*, 418–431.
DOI: 10.1016/j.jhazmat.2007.04.007

Stolz, J., Basu, P., and Oremland, R. (2002). Microbial transformation of elements: the case of arsenic and selenium. International Microbiology *5*, 201–207.
DOI: 10.1007/s10123-002-0091-y

Swallow, K.C., Hume, D.N., and Morel, F.M.M. (1980). Sorption of copper and lead by hydrous ferric oxide. Environmental Science and Technology *14*, 1326–1331.
DOI: 10.1021/es60171a003

Thouin, H., Le Forestier, L., Gautret, P., Hube, D., Laperche, V., Dupraz, S., and Battaglia-Brunet, F. (2016). Characterization and mobility of arsenic and heavy metals in soils polluted by the destruction of arsenic-containing shells from the Great War. Science of The Total Environment *550*, 658–669.

554 DOI: 10.1016/j.scitotenv.2016.01.111

555 Thouin, H., Battaglia-Brunet, F., Gautret, P., Le Forestier, L., Breeze, D., Séby, F., Norini, M.-P., and Dupraz, S.
556 (2017). Effect of water table variations and input of natural organic matter on the cycles of C and N, and mobility
557 of As, Zn and Cu from a soil impacted by the burning of chemical warfare agents: A mesocosm study. Science of
558 The Total Environment *595*, 279–293.
559 DOI: 10.1016/j.scitotenv.2017.03.218

560 Tiedje, J.M., Asuming-Brempong, S., Nüsslein, K., Marsh, T.L., and Flynn, S.J. (1999). Opening the black box of
561 soil microbial diversity. Applied Soil Ecology *13*, 109–122.
562 DOI: 10.1016/S0929-1393(99)00026-8

563 Twidwell, L.G., Plessas, K.O., Comba, P.G., and Dahnke, D.R. (1994). Removal of arsenic from wastewaters and
564 stabilization of arsenic bearing waste solids: Summary of experimental studies. Journal of Hazardous Materials
565 *36*, 69–80.
566 DOI: 10.1016/0304-3894(93)E0054-6

567 Weber F. A., Hofacker A. F., Kretzschmar R. (2010). Temperature dependence and coupling of iron and arsenic
568 reduction and release during flooding of a contaminated soil. Environmental Science and Technology *44*, 116-
569 122.
570 DOI: 10.1021/es902100h

571 Vereš, J. (2014). Determination of zinc speciation in metallurgical wastes by various analytical methods.
572 International Journal, *5*(5).

573 Wolf, M., Lehndorff, E., Wiesenberg, G.L.B., Stockhausen, M., Schwark, L., and Amelung, W. (2013). Towards
574 reconstruction of past fire regimes from geochemical analysis of charcoal. Organic Geochemistry *55*, 11–21.
575 DOI: 10.1016/j.orggeochem.2012.11.002

576 Xiao K.-Q., Li L. G., Ma L. P., Zhang S. Y., Bao P., Zhang T., Zhu Y.-G. (2016). Metagenomic analysis revealed
577 highly diverse microbial arsenic metabolism genes in paddy soils with low-arsenic contents. Environmental
578 Pollution *211*, 1-8.
579 DOI: 10.1016/j.envpol.2015.12.023

580 Yamamura, S., Watanabe, M., Yamamoto, N., Sei, K., and Ike, M. (2009). Potential for microbially mediated
581 redox transformations and mobilization of arsenic in uncontaminated soils. Chemosphere *77*, 169–174.
582 DOI: 10.1016/j.chemosphere.2009.07.071

583 Zobrist, J., Dowdle, P.R., Davis, J.A., and Oremland, R.S. (2000). Mobilization of arsenite by dissimilatory
584 reduction of adsorbed arsenate. Environmental Science and Technology *34*, 4747–4753.
585 DOI: 10.1021/es001068h